ICHRNVI-2010
Date : March. 11, 2010
Place : Waseda

Statistics of Quasi-geostrophic Point Vortices
- Equilibrium of Interacting Vortex Clouds -

Takeshi Miyazaki, Tomoyoshi Sato, Hidefumi Kimura and Naoya Takahashi

The University of Electro-Communications
UEC

Dept. Mech. Eng. Int'l Systems.,
University of Electro-Communications
1-5-1, Chofugaoka, Chofu, Tokyo, 182-8585, Japan

Outline

Background

The relevance of vortices in Geophysical flows

Quasi-geostrophic Approximation

Hierarchy of approximation

Statistical Mechanics of QG Point Vortices (Review)

"Mono-disperse" (All vortices of identical strength)

Numerical Simulation ⟹ "Equilibrium"

Comparison with the "Maximum entropy theory"

and simplified *"2-Parameter Model"*

Influence of vertical vorticity distribution and energy

Vortex Clouds Interaction

Change of vorticity distribution inside the vortex clouds

Influence of External Flow Flied on Equilibrium

Simulations under *"Horizontal Strain", "Vertical Shear"*

"Possible Physical Interpretation"

Background (1)

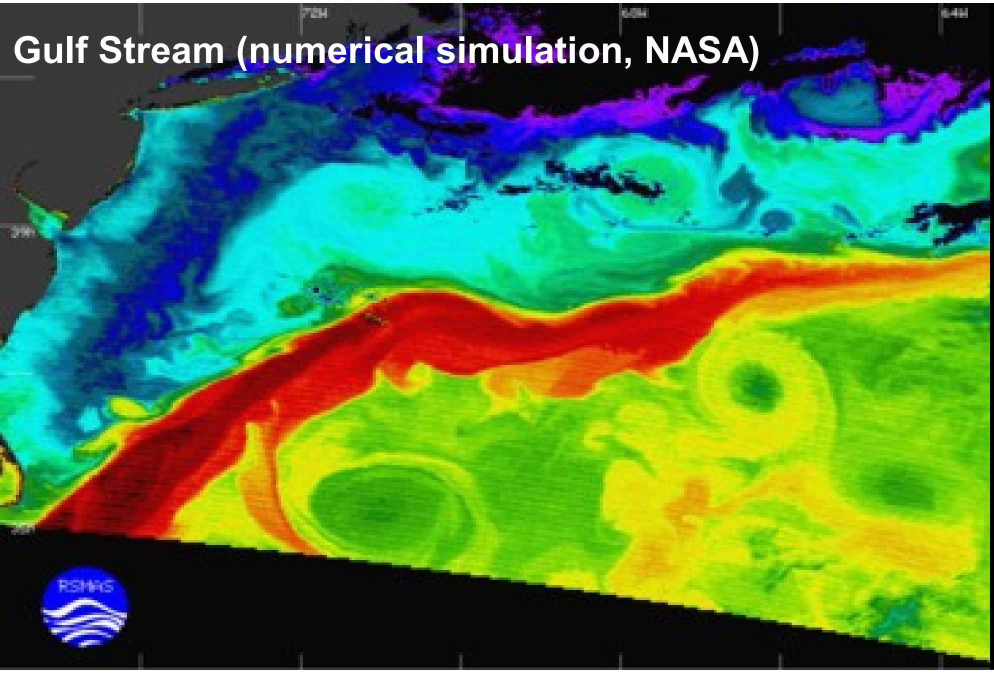
Gulf Stream (numerical simulation, NASA)

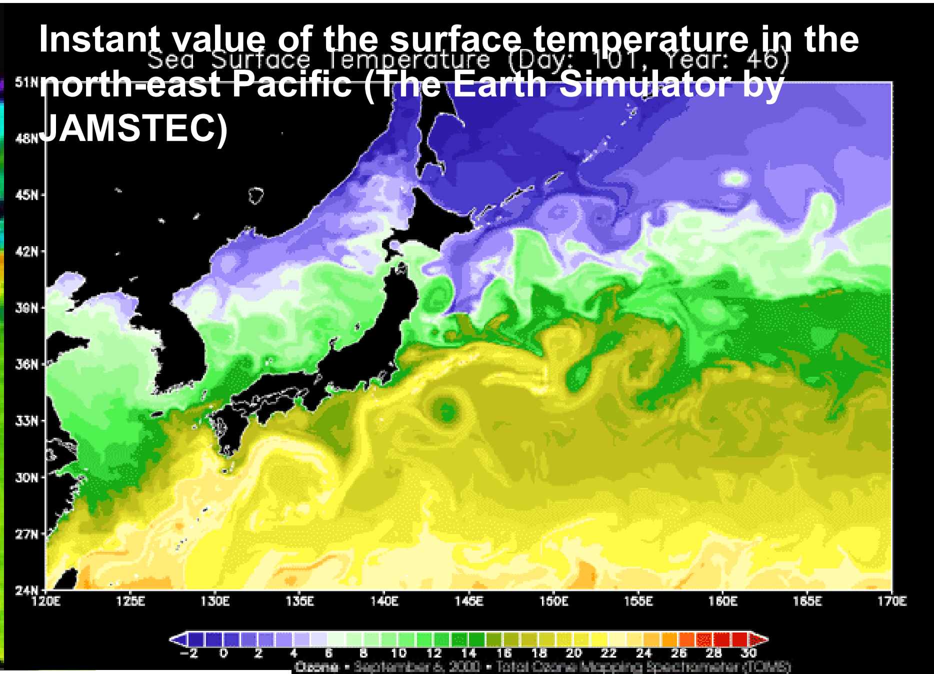

Instant value of the surface temperature in the north-east Pacific (The Earth Simulator by JAMSTEC)

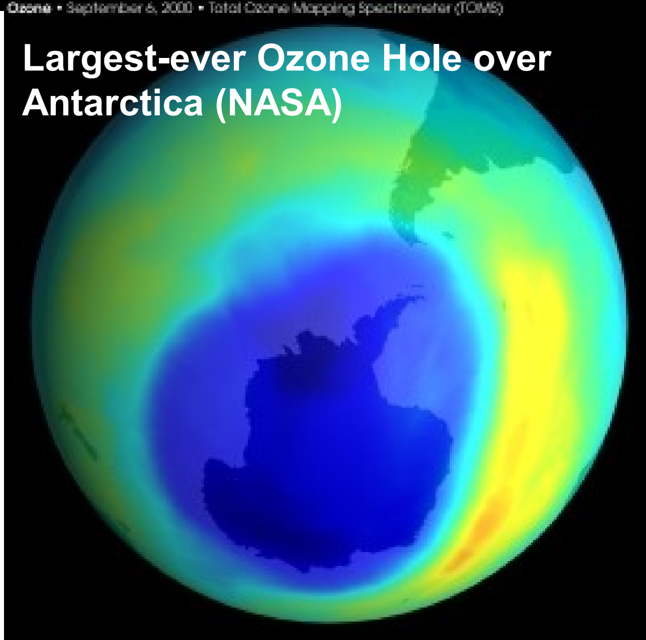

Largest-ever Ozone Hole over Antarctica (NASA)

Geophysical flows …

Vertical motion is suppressed due to the Coriolis force and stable stratification.

In a rotating stratified fluid, the interactions of isolated coherent vortices dominate the turbulence dynamics.

Background (2)

Two-dimensional point vortex systems

lowest order approximation of geophysical flows

- **Many studies** have been made on purely 2D flows.

Statistical mechanics

☑ L. Onsager (1949),
negative temperature

☑ D. Montgomery and G. Joyce (1974),
canonical ensemble

☑ Y. B. Pointin and T. S. Lundgren (1976),
micro canonical ensemble

☑ Yatsuyanagi *et al*. (2005),
very large numerical simulation (N = 6724)

The actual geophysical flows are 3D.

- The fluid motions are almost confined within a horizontal plane
- Different motions are allowed on different horizontal planes.

'Quasi-geostrophic approximation'
(next order approximation)

⇒The QG-approximation confines the motion in different horizontal planes with "interacting" two dimensional behavior.

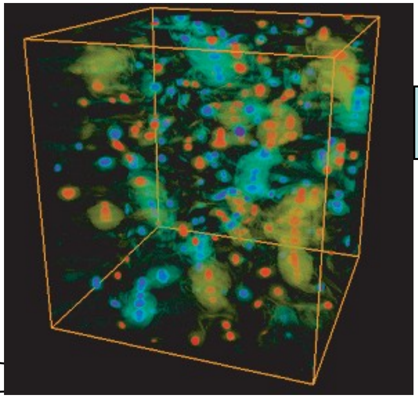

J. C. McWilliams *et al.* (1994)
Coherent vortex structures in QG turbulence

2-layer QG point vortex system (2001)
by Mark T. DiBattista and Andrew J. Majda

Vortex models

Point vortex
N degrees of freedom

Spheroidal vortex
2*N* degrees of freedom
Miyazaki *et al.* (2005)

Ellipsoidal vortex
3*N* degrees of freedom
Li *et al.* (2006)

Quasi-geostrophic Approximation

Fluid motion (Ψ : stream function)

$$u = \frac{\partial \Psi}{\partial y}, \quad v = -\frac{\partial \Psi}{\partial x}, \quad w = O\left(\frac{f_0}{N}\right) \leftarrow \text{negligibly small}$$

$N \fallingdotseq 1.16\times10^{-2}\ \mathrm{s}^{-1}$, $f_0 \sim 1/(24[\mathrm{h}])$

N : **Brunt-Vaisala frequency**

f_0 : **Coriolis parameter** ($f_0 = 2\Omega\sin\theta$ by at latitude θ)

Time-evolution under the quasi-geostrophic approximation

$$\left(\frac{\partial}{\partial t} + \frac{\partial \Psi}{\partial y}\frac{\partial}{\partial x} - \frac{\partial \Psi}{\partial x}\frac{\partial}{\partial y}\right) q = 0$$

Potential vorticity

$$q = -\Delta\Psi = -\left(\frac{\partial^2}{\partial x^2} + \frac{\partial^2}{\partial y^2} + \frac{\partial^2}{\partial z^2}\right)\Psi$$

Point vortex systems($\hat{\Gamma}_i$: strength, $\boldsymbol{R}_i$: location)

$$q = \sum_{i=1}^{N} \hat{\Gamma}_i \delta(\boldsymbol{r} - \boldsymbol{R}_i), \quad \boldsymbol{r} = (x, y, z)$$

Assuming δ-function like concentration at N points, each vortex is advected by the flow field induced by other vortices.

Equation of Motion for Quasi-geostrophic Point Vortices

Canonical Variables : X, Y, Z

Hamiltonian of QG *N* point vortex system (invariant)

$$H = \sum_{(i,j)}^{N} H_{mij}, \quad H_{mij} = \frac{\hat{\Gamma}_i \hat{\Gamma}_j}{4\pi |\boldsymbol{R}_i - \boldsymbol{R}_j|}$$

interaction energy

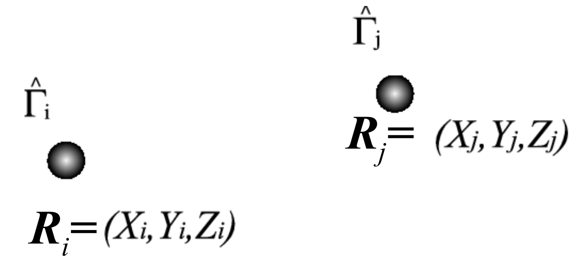

Canonical equations of motion for the ***i*−th** vortex

$$\frac{\mathrm{d}X_i}{\mathrm{d}t} = \frac{1}{\hat{\Gamma}_i}\frac{\partial H}{\partial Y_i}, \qquad \frac{\mathrm{d}Y_i}{\mathrm{d}t} = -\frac{1}{\hat{\Gamma}_i}\frac{\partial H}{\partial X_i}$$

Computation on MDGRAPE-3 Special Purpose Computer &
Time Integration with LSODE (6 significant digits)

t : dimensionless time (in units of the inverse potential vorticity)

Center of the Vorticity (invariant) : shift the coordinate origin to the vorticity center

$$P = \sum_{i=1}^{N} \hat{\Gamma}_i X_i \Big/ \sum_{i=1}^{N} \hat{\Gamma}_i = 0, \quad Q = \sum_{i=1}^{N} \hat{\Gamma}_i Y_i \Big/ \sum_{i=1}^{N} \hat{\Gamma}_i = 0$$

Angular momentum (invariant)

$$I = \sum_{i=1}^{N} \hat{\Gamma}_i (X_i^2 + Y_i^2) = \sum_{i=1}^{N} \hat{\Gamma}_i \Rightarrow$$

Length scale is normalized by I .

Poisson commutable invariants : P^2+Q^2, I, H $\Rightarrow$ Chaotic behavior
(According to the Liouville-Arnol'd theorem)

Computer simulation & Statistical theory

MDGRAPE-3

© http://mdgrape.gsc.riken.jp

Specifications

Number of MFGRAPE-3 Chip : 2
Performance : 330 Gflops (peak)
Host Interface : PCI-X 64bit/100MHz
Power Consumption : 40 W

The architecture of MDGRAPE-3 is quite similar to its predecessors, the GRAPE (GRAvity PipE) systems. The GRAPE systems are special-purpose computers for gravitational *N*-body simulations and molecular dynamics simulations developed in University of Tokyo. Its predecessor MDM (Molecular Dynamics Machine), developed by RIKEN, achieved 78 Tflops peak performance in 2000. The GRAPE systems won seven Gordon Bell prizes in total.
It consists of 20 force calculation pipelines, a j-particle memory unit, a cell-index controller, a master controller, and a force summation unit.

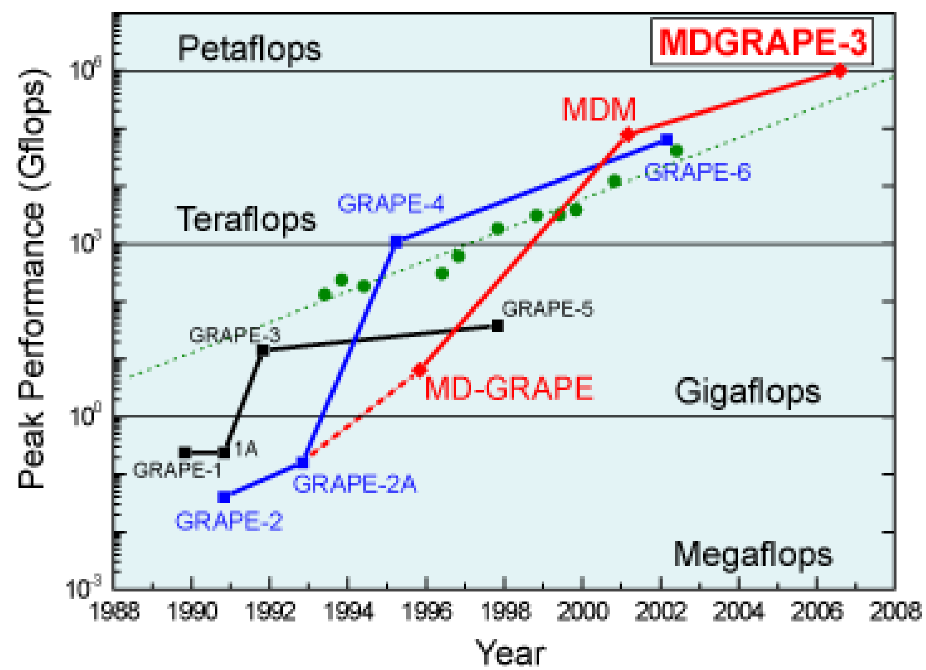

Temperature in Statistical Mechanics

- Random initial distributions (10^6 ensembles)

◆ **Case B** : Positive Temperature
($E=3.054\times10^{-2}$)

◆ **Case A** : 0-Inverse-Temperature
($E=3.130\times10^{-2}$)

◆ **Case C** : Negative Temperature
($E=3.236\times10^{-2}$)

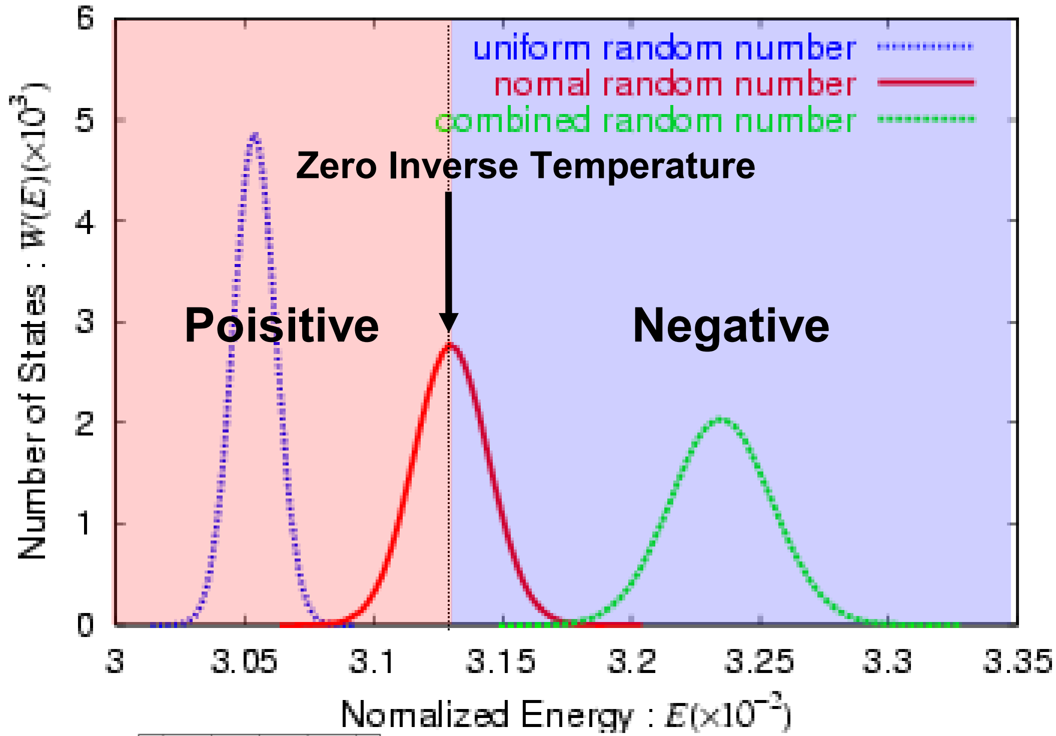

Initial Distribution

Uniform

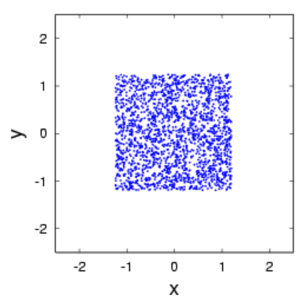
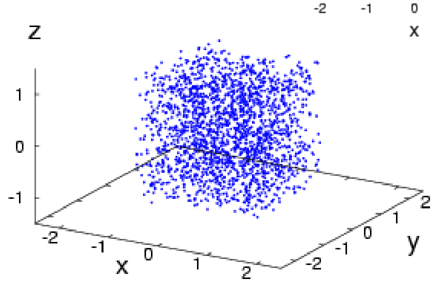

Normal

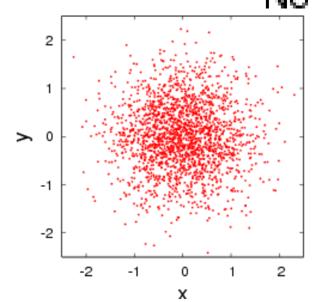
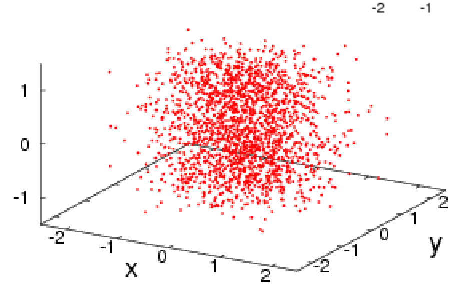

Combined

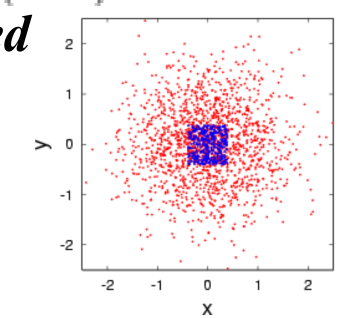
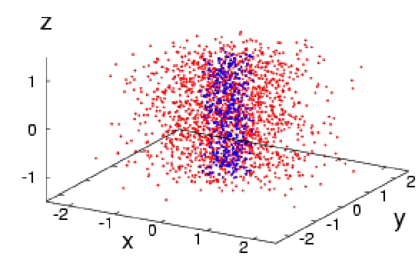

Influence of the Energy

Equilibrium

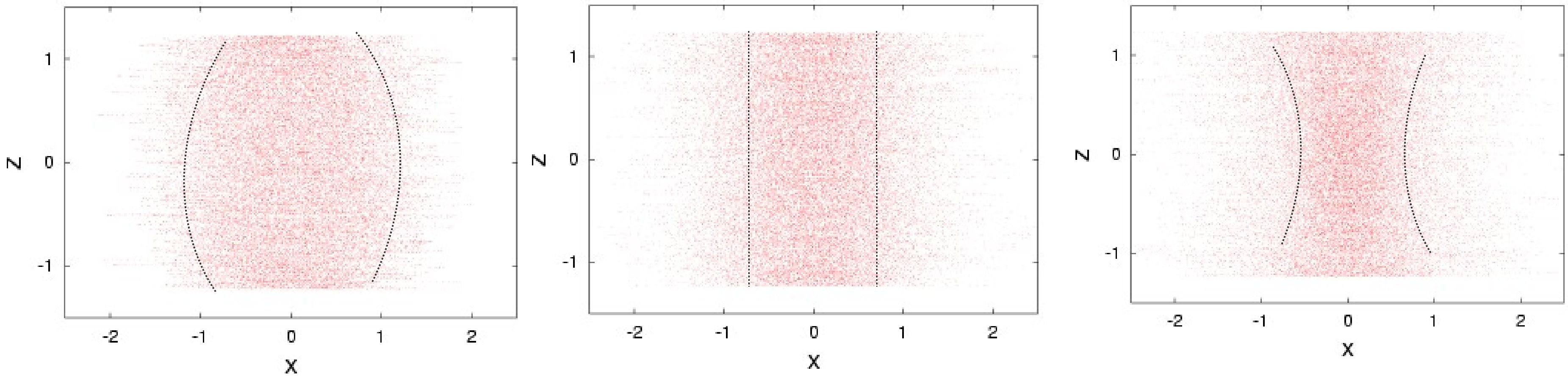

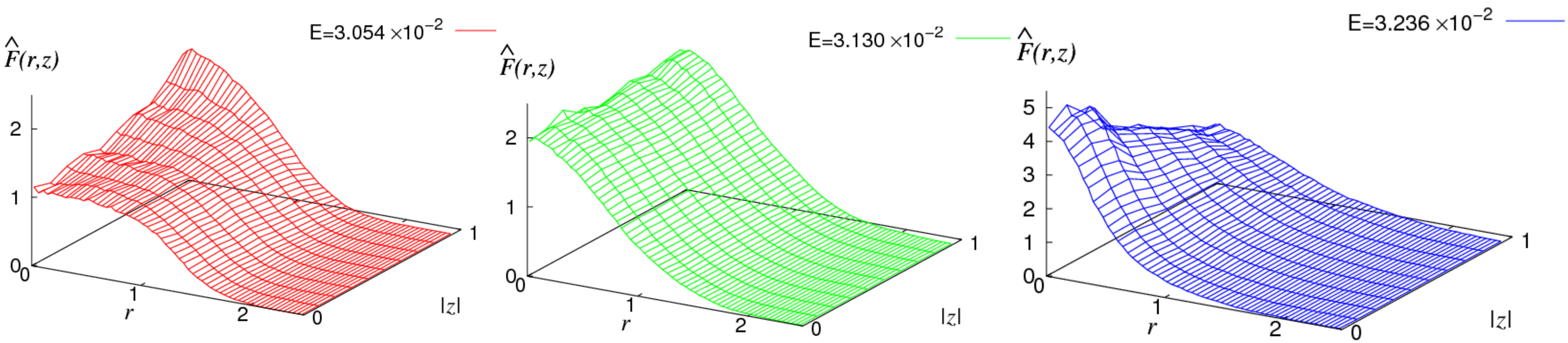

Case B **Case A** **Case C**

<u>Case B</u>

"End-effect" ･･･Tighter concentration around the axis at the upper and lower lids

<u>Case C</u>

"Inverse-end-effect" ･･･ Tighter concentration around the axis in the center region (z=0)

Influence of the Energy (Two-parameter Fitting)

PDF: $$F(r,z) = \frac{k(z)P(z)}{2\pi a^2(z)\Gamma(\frac{2}{k(z)})} e^{-(\frac{r}{a(z)})^{k(z)}}$$

$a(z) = 1$, $k(z) = 2$ ⇨ Gaussian

$k(z) = \infty$ ⇨ Top-hat

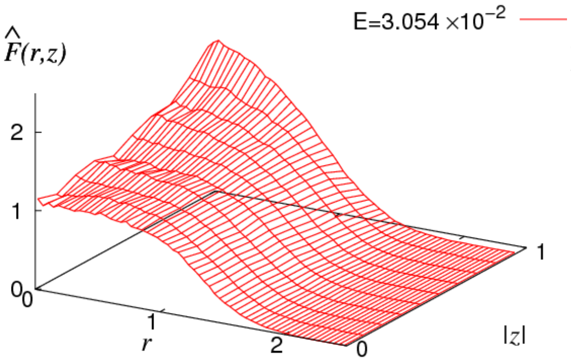

Case B

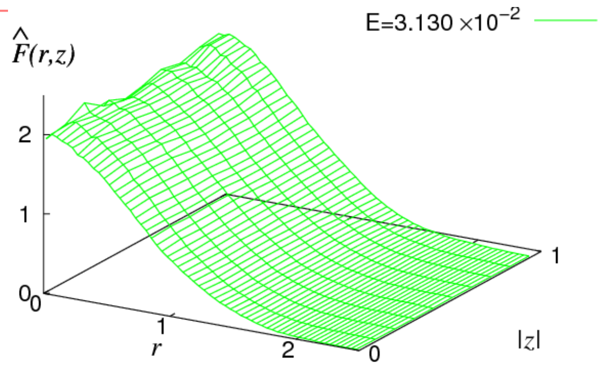

Case A

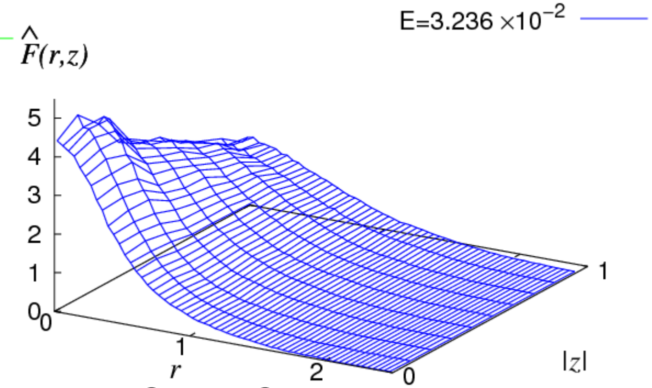

Case C

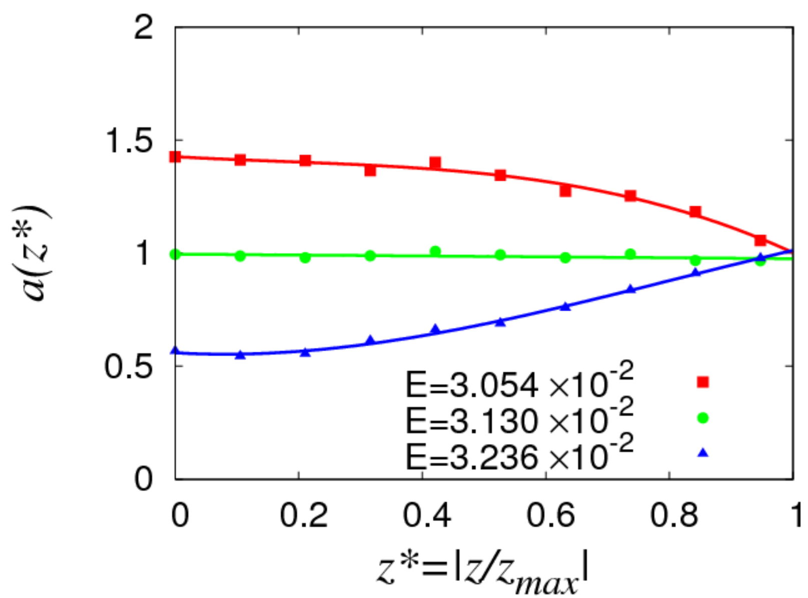

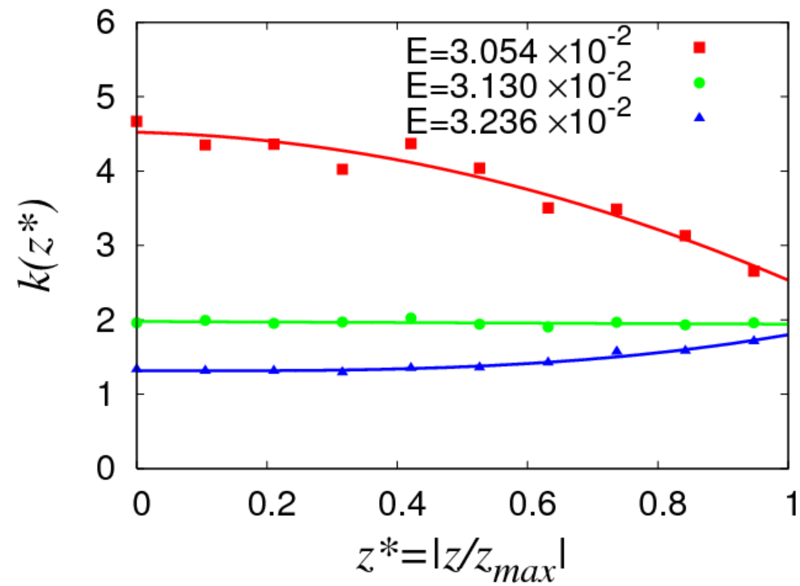

Physical Interpretation

Concentrated more closely
around the axis of symmetry

Energy-increase (minor)
Entropy-decrease
A-momentum-decrease

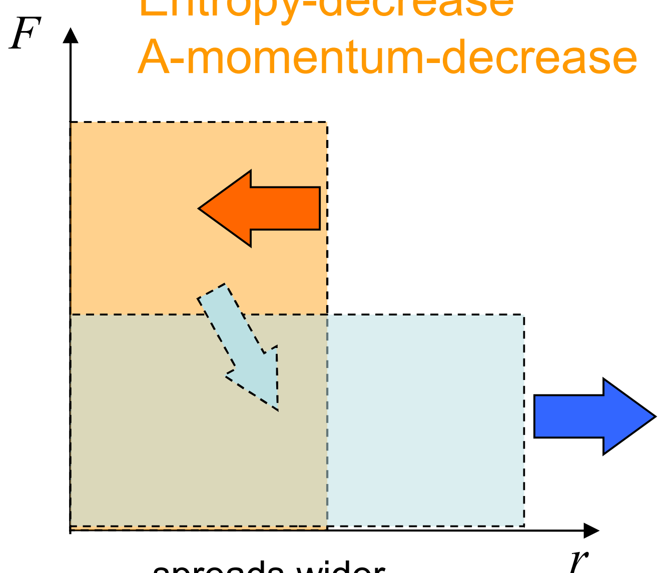

spreads wider
(constrained by **angular momentum**)

Energy-decrease (major)
Entropy-increase
A-momentum-increase

- The distribution in the center region expands radially for lower energy and shrinks for higher energy.

- In order to keep the angular momentum unchanged, the distribution near the lids should shrink for lower energy and should expand for higher energy.

Influence of the Vertical Vorticity Distribution

✓ Parabolic vertical distribution like an ellipsoidal vortex patch

$$\boxed{P(z) = \frac{3}{4z_{max}}\left(1 - \frac{z^2}{{z_{max}}^2}\right)}$$

c.f. Top-hat

$$P(z) = \frac{1}{2z_{\max}} = const.$$

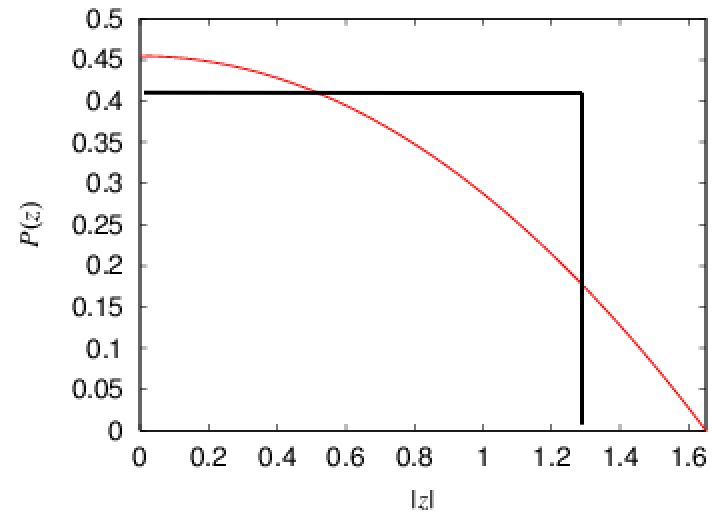

- **Case E1**
  - **Positive temperature**
  - **E =3.019×10^-2**
- **Case E2**
  - **0-inverse-temperature**
  - **E =3.133×10^-2**
- **Case E3**
  - **Negative temperature**
  - **E =3.260×10^-2**

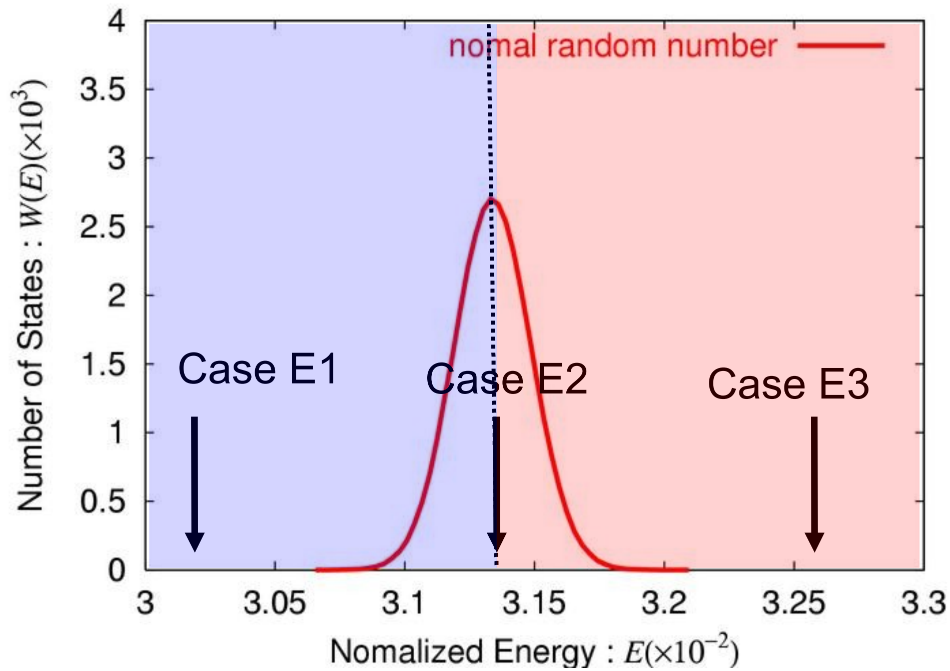

Influence of the Energy (Parabolic Case)

PDF : $$F(r,z) = \frac{k(z)P(z)}{2\pi a^2(z)\Gamma(\frac{2}{k(z)})} e^{-(\frac{r}{a(z)})^{k(z)}}$$

$a(z) = 1$, $k(z) = 2$ ⇨ Gaussian

$k(z) = \infty$ ⇨ Top-hat

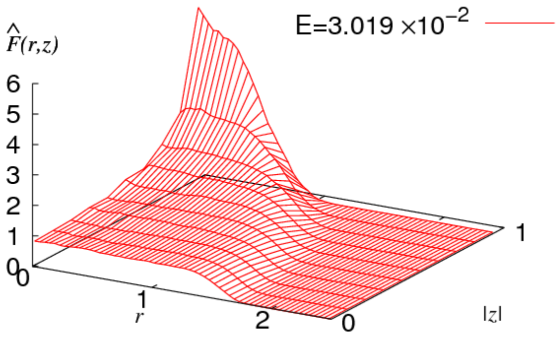

Case E1

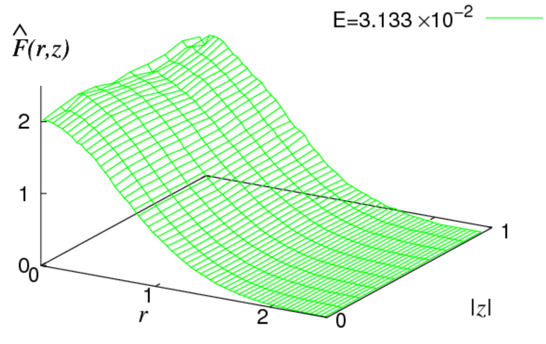

Case E2

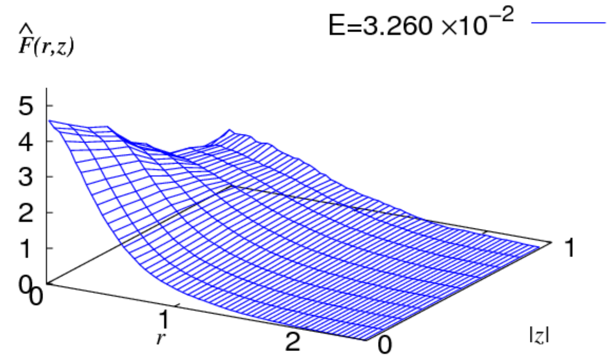

Case E3

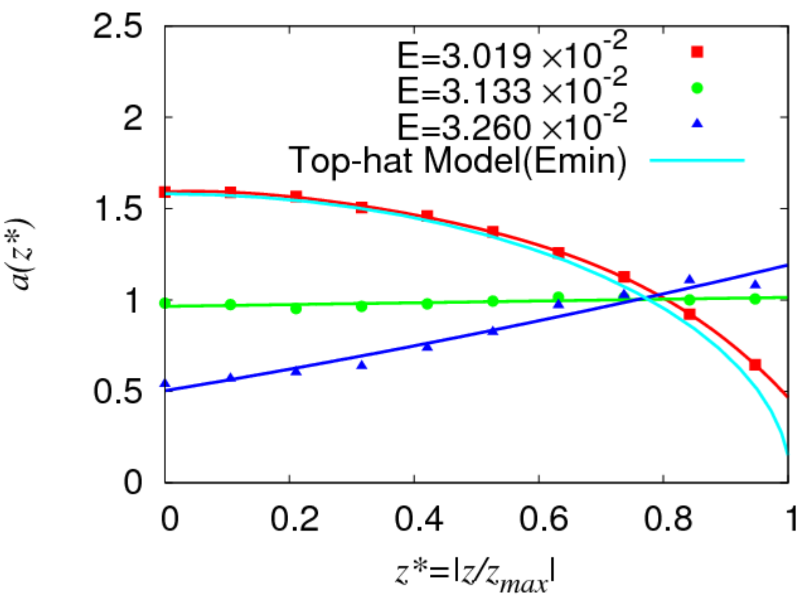

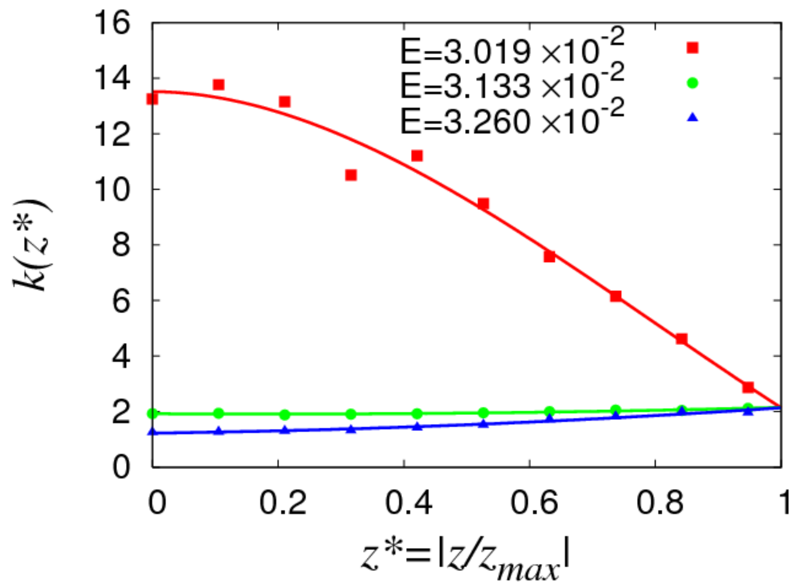

Maximum Entropy Theory: Mono-disperse System

Two-dimensional point vortices by Kida (J. P. S. J., **39**(5) (1975), pp.1395-1404)

$F(\boldsymbol{r})$: Probability density function

Shannon entropy

$$\log \hat{Z} = -\hat{N} \iiint F(\boldsymbol{r}) \log F(\boldsymbol{r}) d^3\boldsymbol{r}$$

Maximize $\hat{Z}$

under the constraints of fixed $P(z)$, I and H.

Vertical distribution of vortices

$$P(z) = \iint F(\boldsymbol{r}) dx dy \quad \left(\int_{z_1}^{z_2} P(z) dz = 1 \right)$$

Angular momentum

$$\hat{I} = \iiint (x^2 + y^2) F(\boldsymbol{r}) d^3\boldsymbol{r} = 1$$

Energy

$$\frac{8\pi H}{\hat{N}^2} = \iiiint\!\!\iint \frac{F(\boldsymbol{r})F(\boldsymbol{r}')}{|\boldsymbol{r} - \boldsymbol{r}'|} d^3\boldsymbol{r} d^3\boldsymbol{r}'$$

$$\log F(\boldsymbol{r}) + 1 + \alpha(z) + \beta(x^2 + y^2) + \frac{\gamma}{4\pi} \iiint \frac{F(\boldsymbol{r}')}{|\boldsymbol{r} - \boldsymbol{r}'|} d^3\boldsymbol{r}' = 0$$

Lagrange multipliers of the Maximum Entropy optimization : $\alpha(z)$, β, γ

Numerical Results vs Maximum Entropy Theory

Hoshi, S. and Miyazaki, T., *FDR* (2008)

‘0-inverse-temperature’

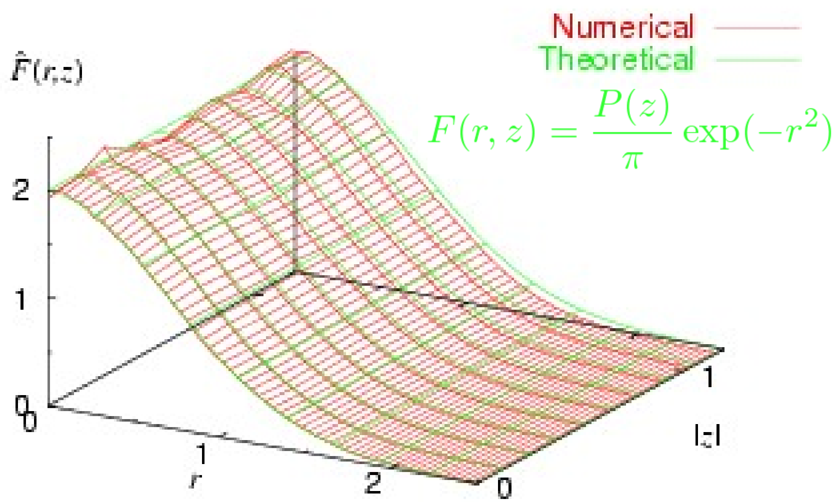

Positive temperature

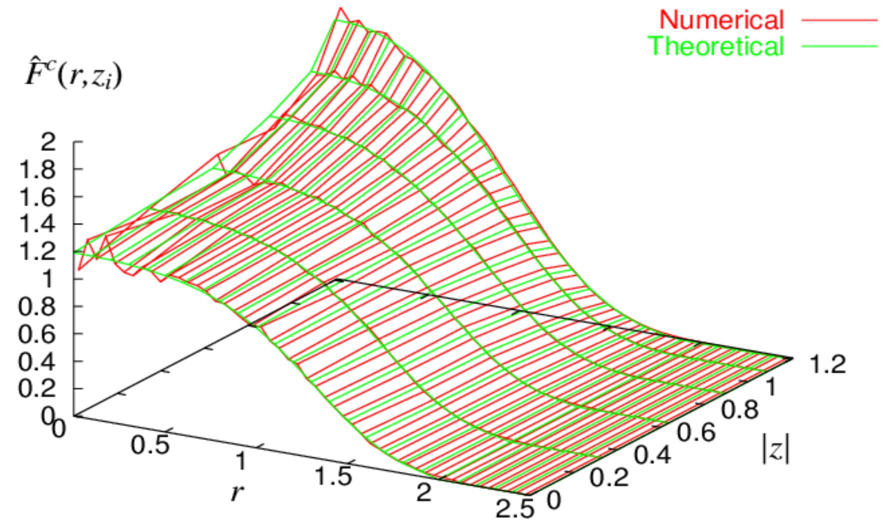

Equilibrium is a maximum entropy state.
(but very difficult to have a well converged solution)

Two Parameter Model

Maximum Entropy Theory: Two-parameter Model

Probability distribution:

$$F(r,z) = \frac{k(z)P(z)}{2\pi a^2(z)\Gamma(\frac{2}{k(z)})} e^{-(\frac{r}{a(z)})^{k(z)}}$$

$a(z)$: radius

$k(z)$: exponent

Angular momentum:

$$I = \int P(z) \frac{a^2(z)\Gamma(\frac{4}{k(z)})}{\Gamma(\frac{2}{k(z)})} dz$$

Energy:

$$H = \frac{N^2\Gamma^2}{4\pi^2} \int \frac{k(z)P(z)}{a^2(z)\Gamma(\frac{2}{k(z)})} dz \int \frac{k(z')P(z')}{a^2(z')\Gamma(\frac{2}{k(z')})} dz$$

$$\times \int_0^\infty r dr \int_0^\infty r' dr' \times \frac{e^{-(\frac{r}{a(z)})^{k(z)}} e^{-(\frac{r'}{a(z')})^{k(z')}}}{\sqrt{(r+r')^2 + (z-z')^2}} \times K\left(\sqrt{\frac{4rr'}{(r+r')^2 + (z-z')^2}}\right)$$

Shannon entropy

$$\log \hat{Z} = -N \int dz P(z) \left[\log\left(\frac{k(z)P(z)}{2\pi a^2(z)\Gamma(\frac{2}{k(z)})}\right) - \frac{2}{k(z)} \right]$$

Maximize the Shannon entropy under these constraints

Two-parameter Model (2)

δa-variation

$$a^2(z)\Gamma(\frac{2}{k(z)}) - \beta a^4(z)\Gamma(\frac{4}{k(z)}) - \gamma k(z)\int dz' \frac{k(z')P(z')}{a^2(z')\Gamma(\frac{2}{k(z')})}\int_0^\infty r dr\int_0^\infty r' dr'$$

$$\times\left[-2 + k(z)(\frac{r}{a(z)})^{k(z)}\right]\frac{e^{-(\frac{r}{a(z)})^{k(z)}}e^{-(\frac{r'}{a(z')})^{k(z')}}}{\sqrt{(r+r')^2+(z-z')^2}}\times K\left(2\sqrt{\frac{rr'}{(r+r')^2+(z-z')^2}}\right) = 0.$$

δk- variation

$$\left(k(z)+2+\frac{2\Gamma'(\frac{2}{k(z)})}{\Gamma(\frac{2}{k(z)})}\right) + 2\beta\frac{a^2(z)\Gamma(\frac{4}{k(z)})}{\Gamma(\frac{2}{k(z)})}\left[\frac{\Gamma'(\frac{2}{k(z)})}{\Gamma(\frac{2}{k(z)})} - \frac{2\Gamma'(\frac{4}{k(z)})}{\Gamma(\frac{4}{k(z)})}\right] + 2\gamma k(z)\frac{1}{\Gamma(\frac{2}{k(z)})}\left\{\left(k(z)+\frac{2\Gamma'(\frac{2}{k(z)})}{\Gamma(\frac{2}{k(z)})}\right)\right.$$

$$\times\int\frac{k(z')P(z')}{a^2(z')\Gamma(\frac{2}{k(z')})}dz'\int_0^\infty r dr\int_0^\infty r' dr'\frac{e^{-(\frac{r}{a(z)})^{k(z)}}e^{-(\frac{r'}{a(z')})^{k(z')}}}{\sqrt{(r+r')^2+(z-z')^2}}\times K\left(2\sqrt{\frac{rr'}{(r+r')^2+(z-z')^2}}\right)$$

$$+k^2(z)\int\frac{k(z')P(z')}{a^2(z')\Gamma(\frac{2}{k(z')})}dz'\int_0^\infty r\log(\frac{a(z)}{r})(\frac{r}{a(z)})^{k(z)}dr\int_0^\infty r' dr'\times\frac{e^{-(\frac{r}{a(z)})^{k(z)}}e^{-(\frac{r'}{a(z')})^{k(z')}}}{\sqrt{(r+r')^2+(z-z')^2}}$$

$$\left.\times K\left(2\sqrt{\frac{rr'}{(r+r')^2+(z-z')^2}}\right)\right\} = 0.$$

Two-parameter Model vs Numerical Results

◆Two-parameter Model

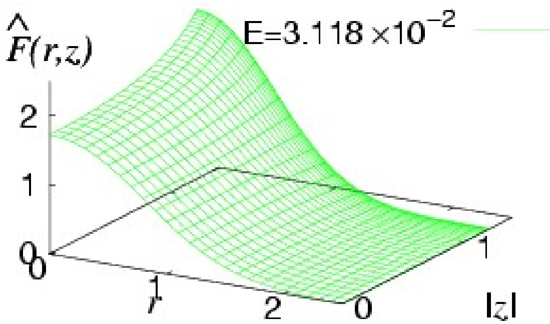

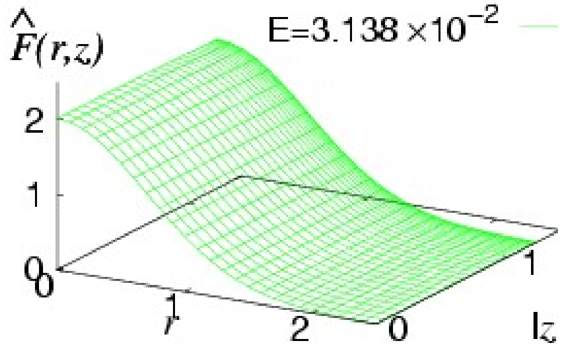

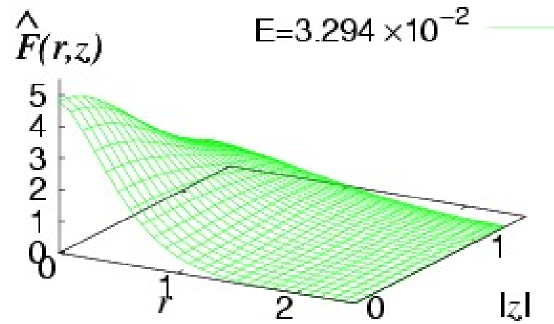

◆**Numerical**

Energy

Case B < Case A < Case C

3.054×10^{-2} 3.130×10^{-2} 3.236×10^{-2}

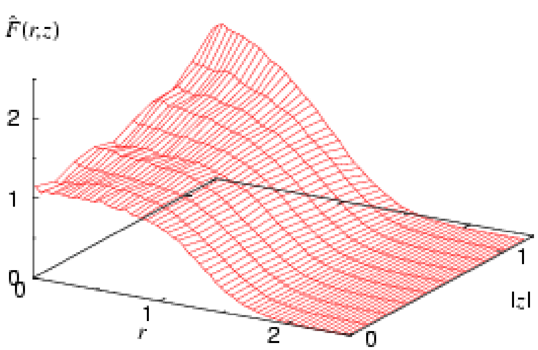

Case B

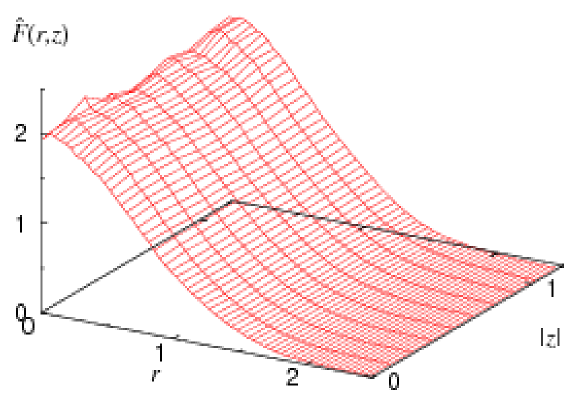

Case A

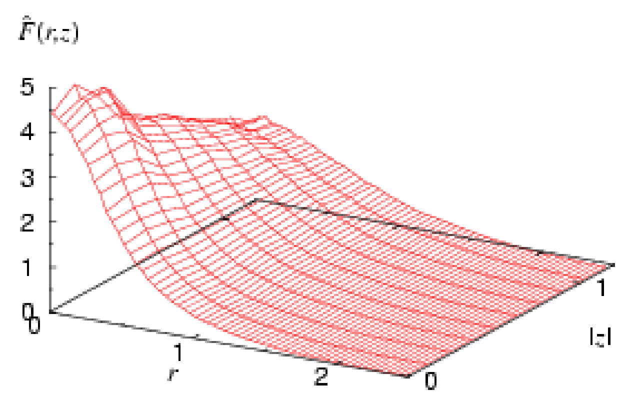

Case C

Two-parameter Model vs Numerical Results

◆Two-parameter Model

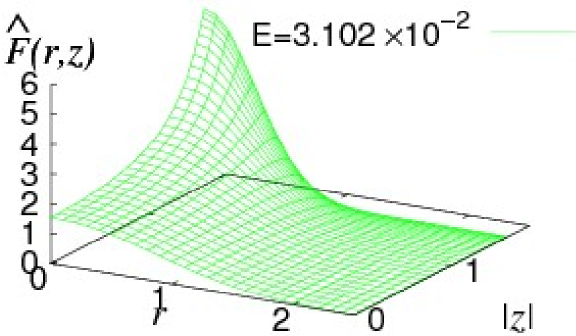

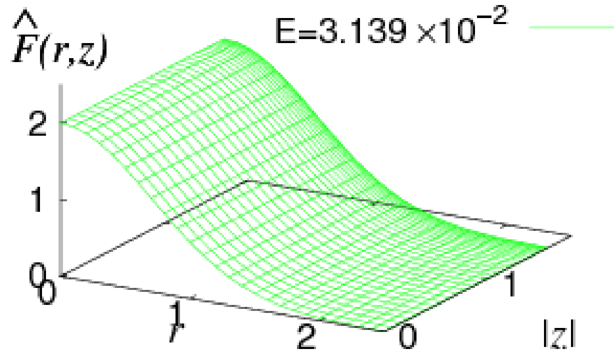

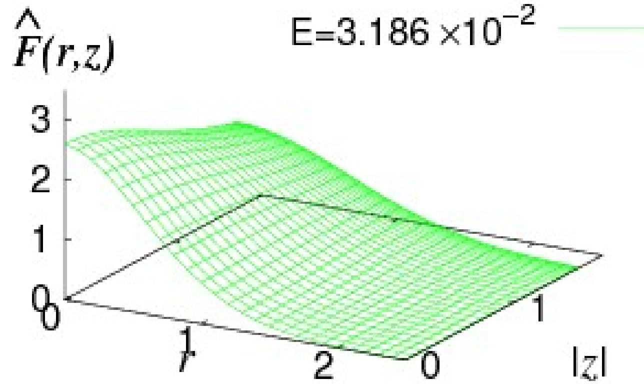

◆**Numerical**

Energy
Case D< Case E < Case F
3.019×10^{-2} 3.133×10^{-2} 3.260×10^{-2}

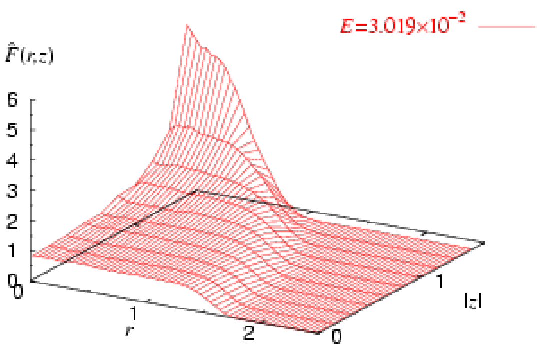

Case D

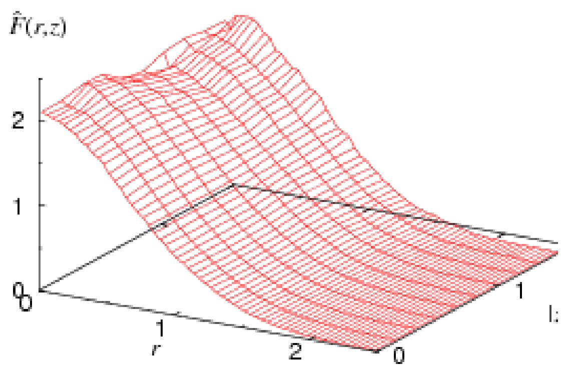

Case E

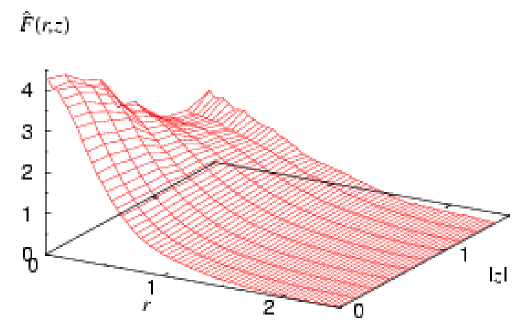

Case F

Interaction between Vortex Clouds: Vorticity Exchange

Two Spheres: $R_1=R_2=1.58$, $D= 5.38$

Top View

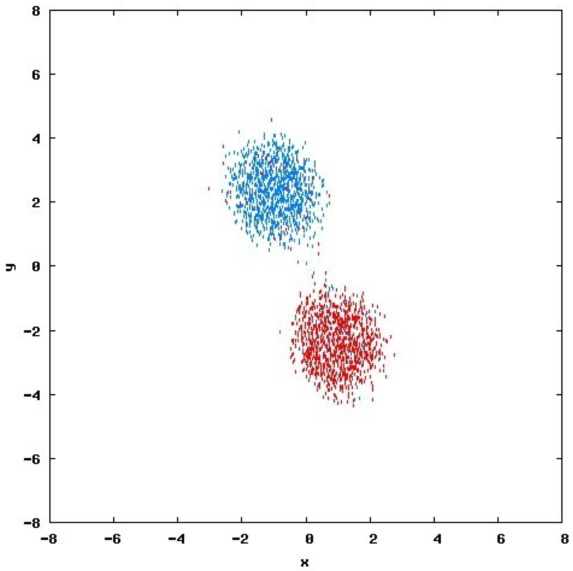

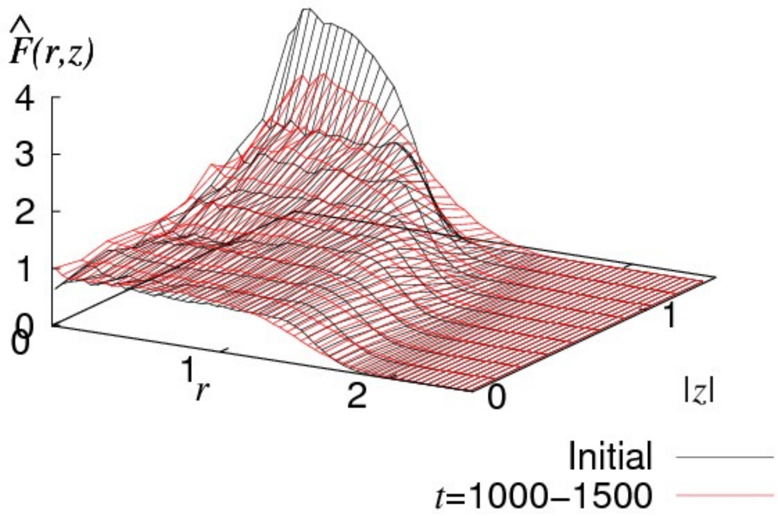

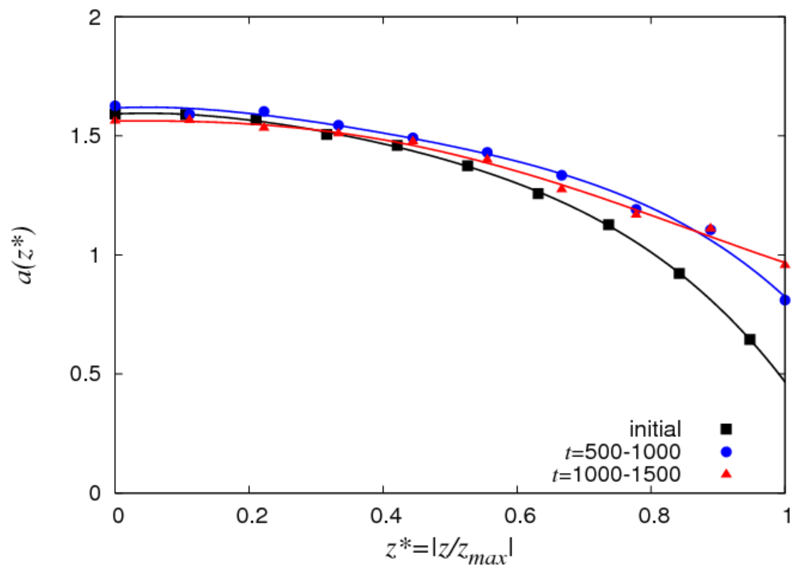

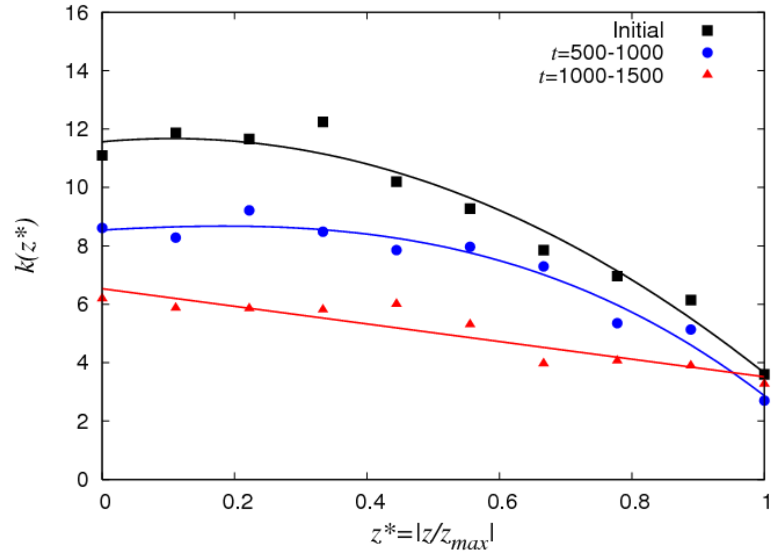

Interaction between Vortex Clouds: Full Merger

Two Spheres: $R_1=R_2=1.58$, $D= 4.11$

Top View

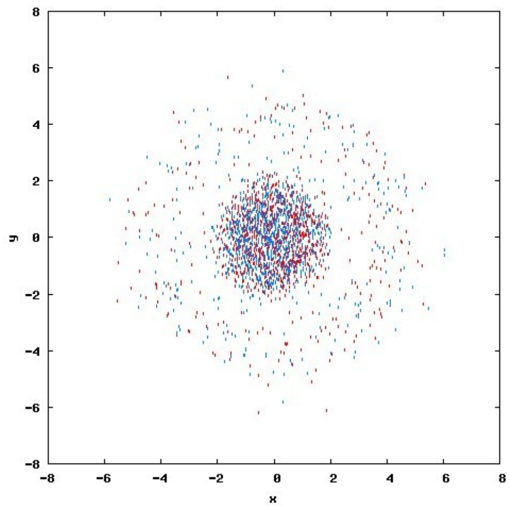

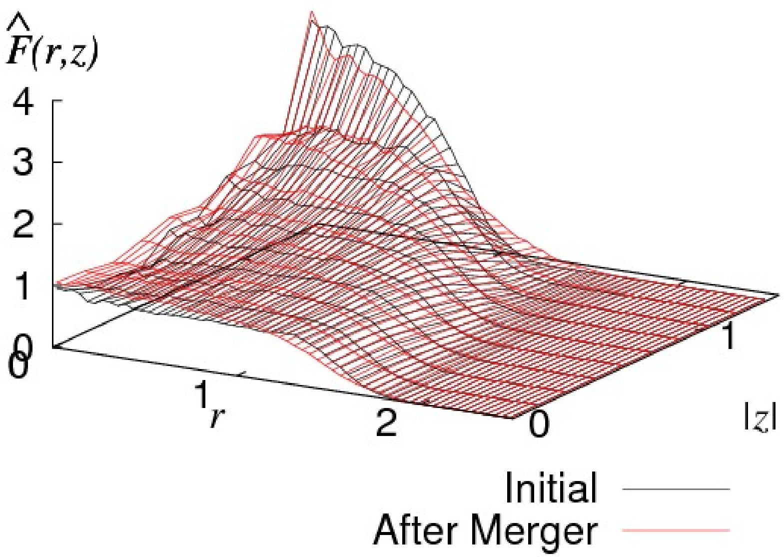

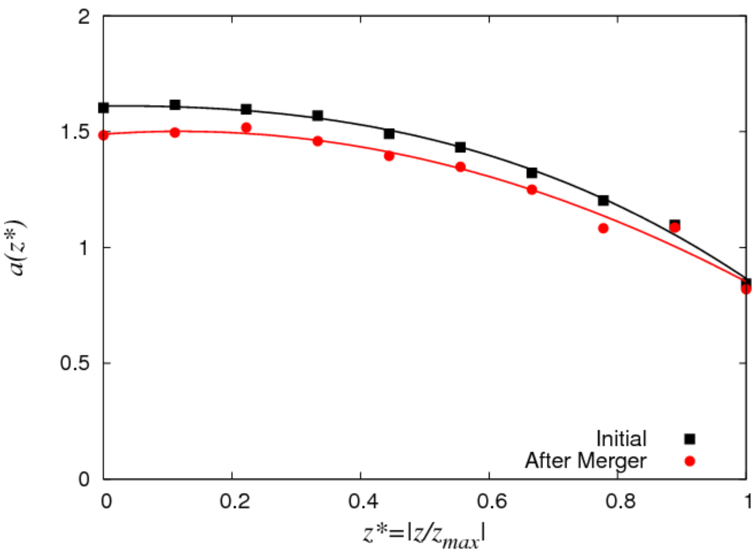

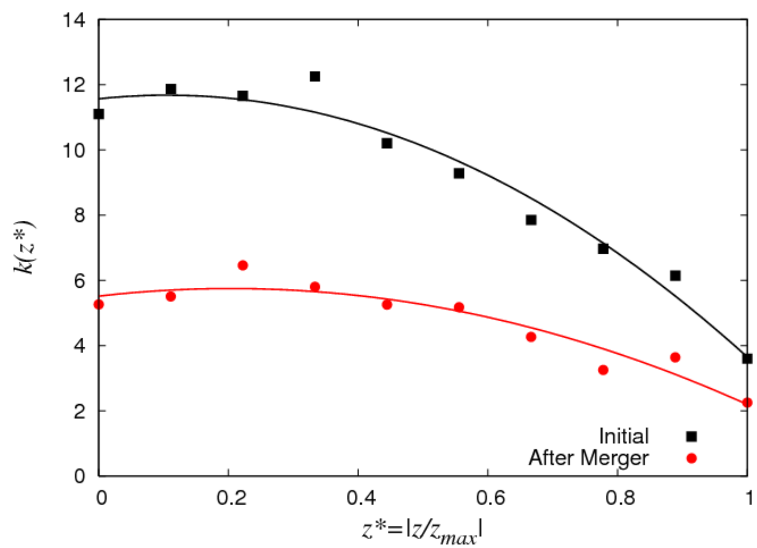

Horizontal Strain and Vertical Shear

Horizontal strain

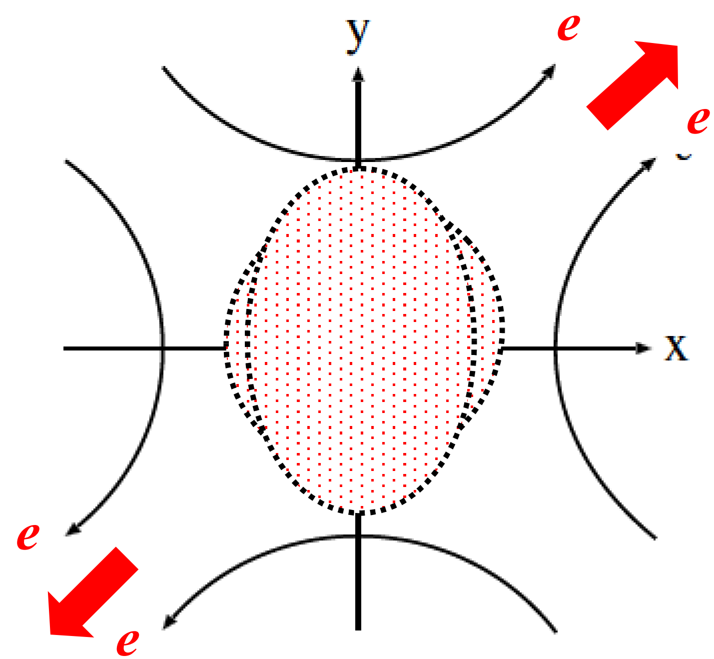

Vertical shear

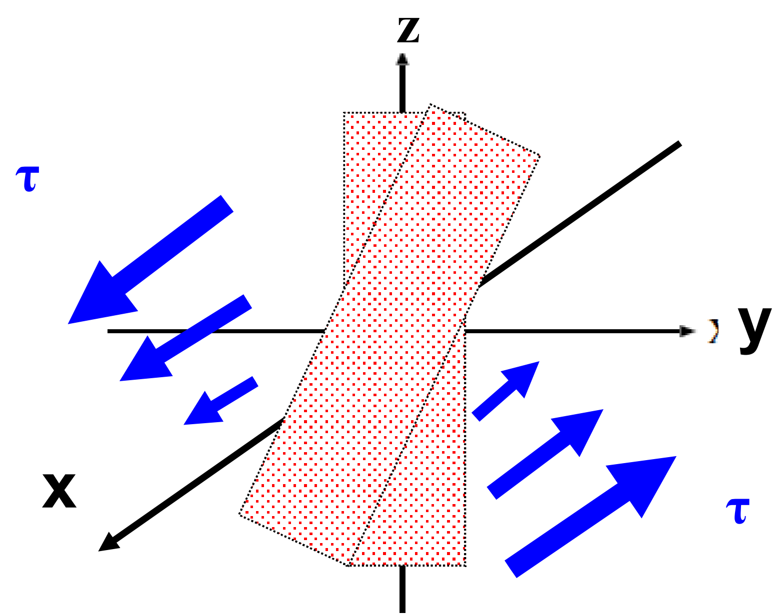

Strain terms

$$H = \sum_{(i,j)}^{N} [H_{mij} + H_e], \quad H_e = \frac{e\hat{\Gamma}_i(-X_i^2 + Y_i^2)}{2}$$

$$\frac{\partial X_i}{\partial t} = \frac{1}{\hat{\Gamma}_i}\frac{\partial H_{mij}}{\partial Y_i} + \underline{eY_i}, \quad \frac{\partial Y_i}{\partial t} = -\frac{1}{\hat{\Gamma}_i}\frac{\partial H_{mij}}{\partial X_i} + \underline{eX_i}$$

Shear term

$$H = \sum_{(i,j)}^{N} [H_{mij} + H_\tau], \quad H_\tau = \tau\hat{\Gamma}_i Y_i Z_i$$

$$\frac{\partial X_i}{\partial t} = \frac{1}{\hat{\Gamma}_i}\frac{\partial H_{mij}}{\partial Y_i} + \underline{\tau Z_i}, \quad \frac{\partial Y_i}{\partial t} = -\frac{1}{\hat{\Gamma}_i}\frac{\partial H_{mij}}{\partial X_i}.$$

Horizontal Strain: Positive Temperature

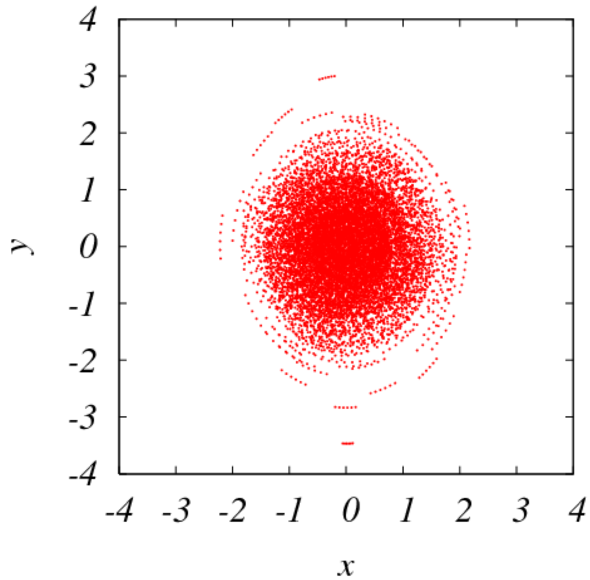

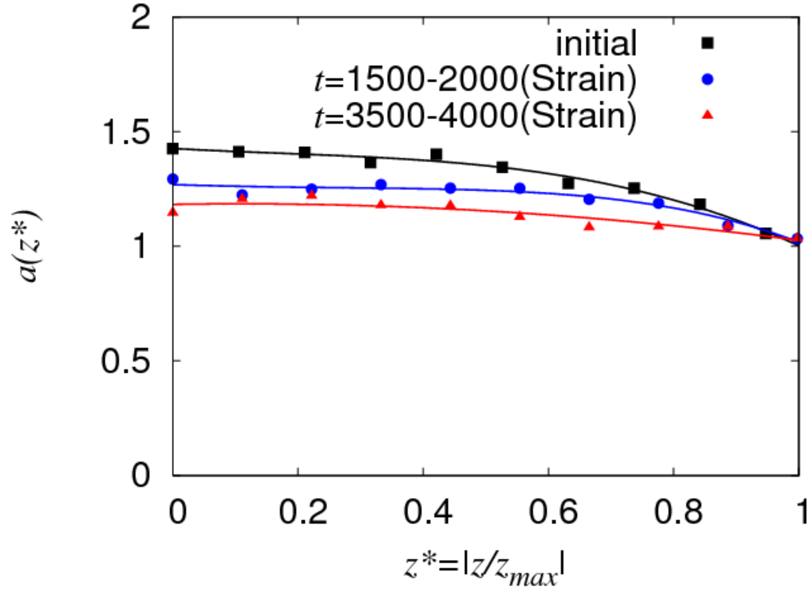

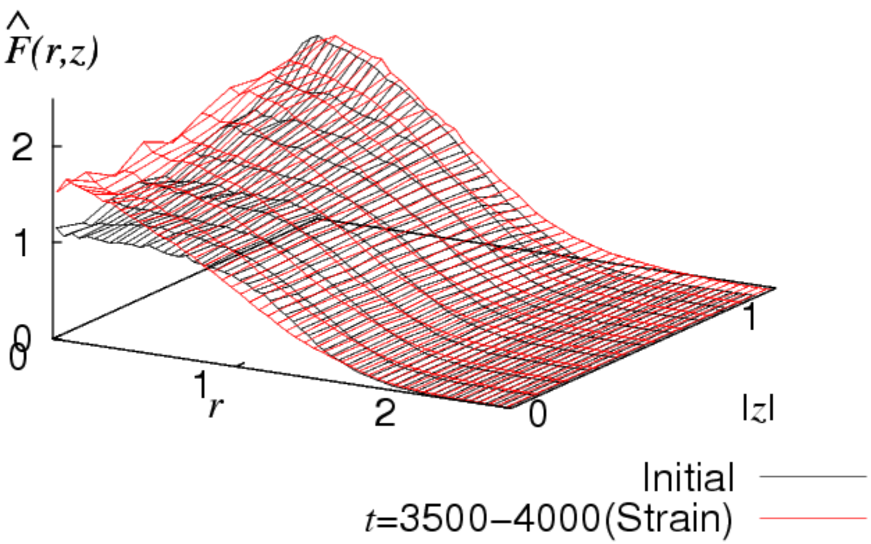

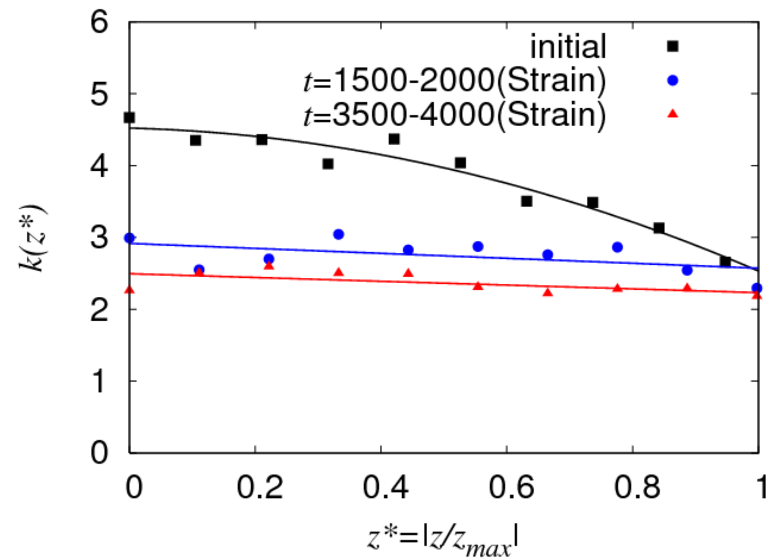

Horizontal Strain: ’0’-inverse Temperature

Initial distribution： ‘0’-inverse temperature

Strain： *e = 0.08*

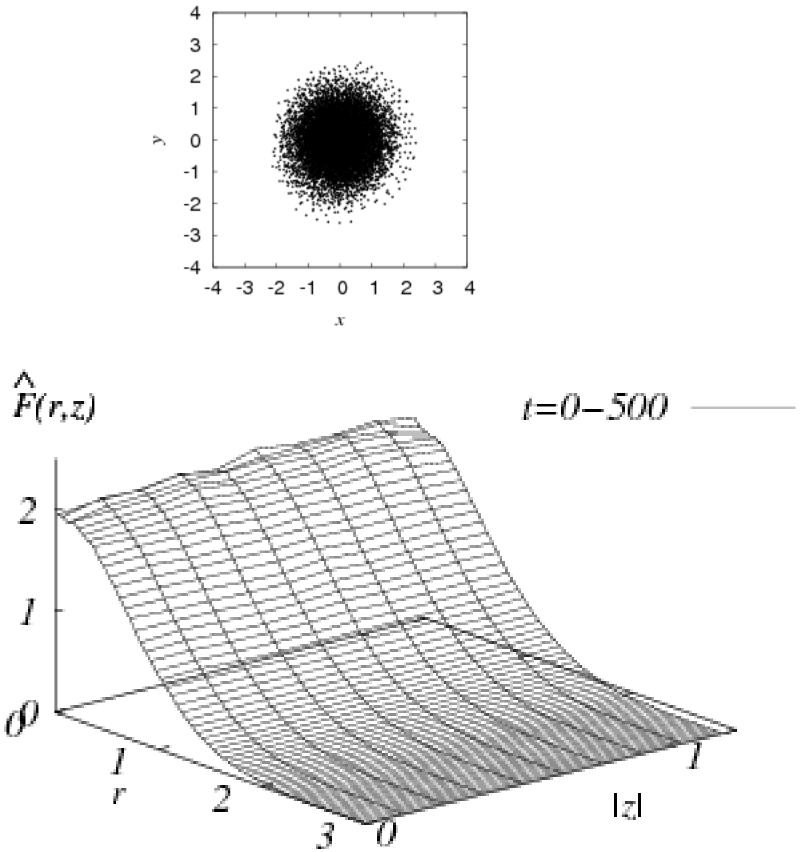

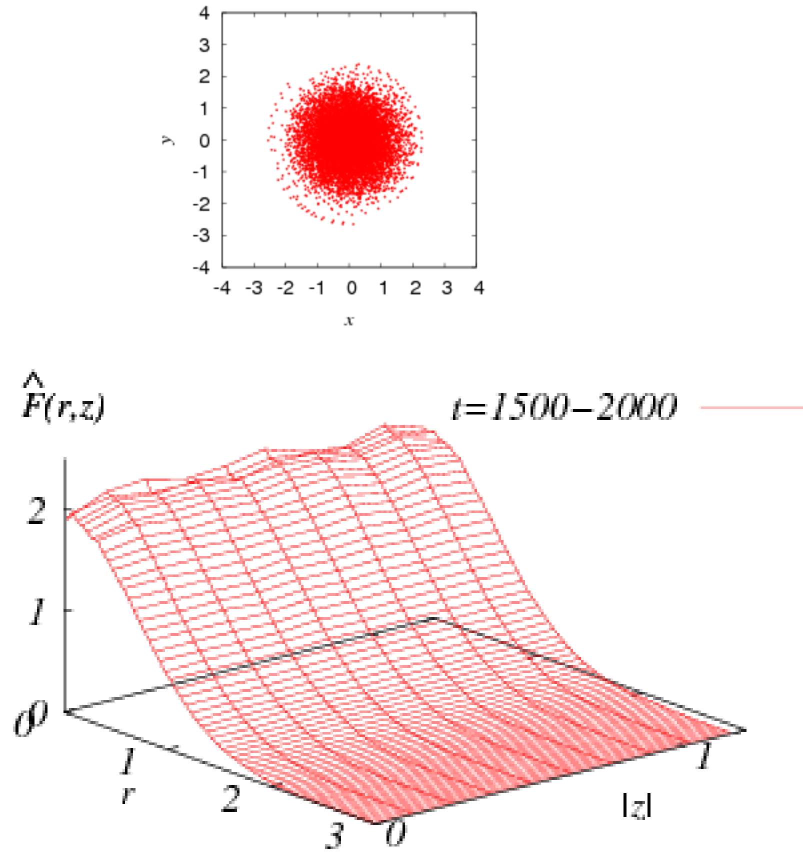

Horizontal Strain: Negative Temperature

Initial distribution ：Negative temperature

Strain ： *e = 0.16*

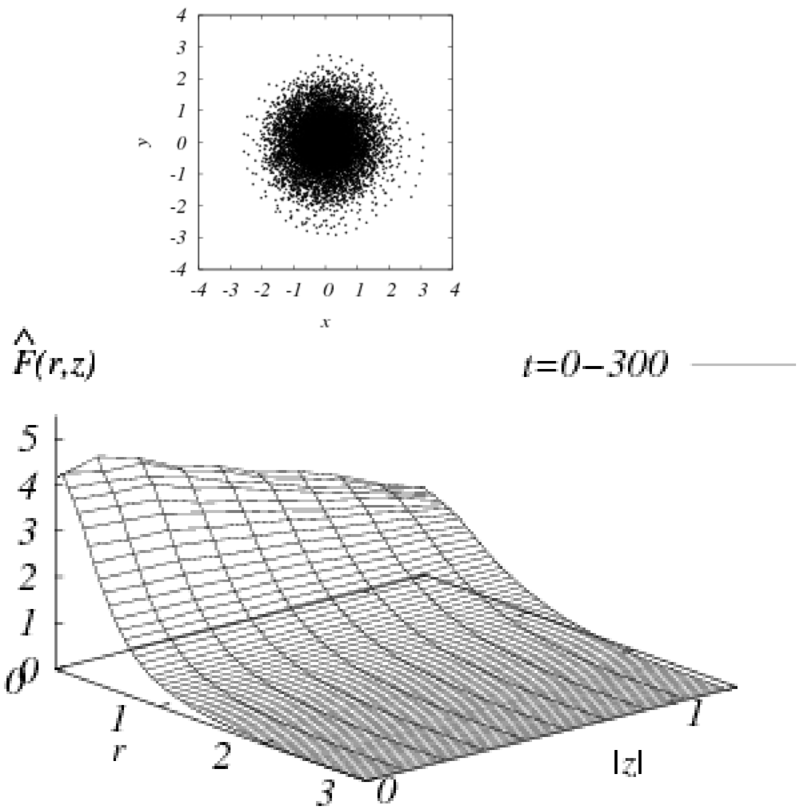

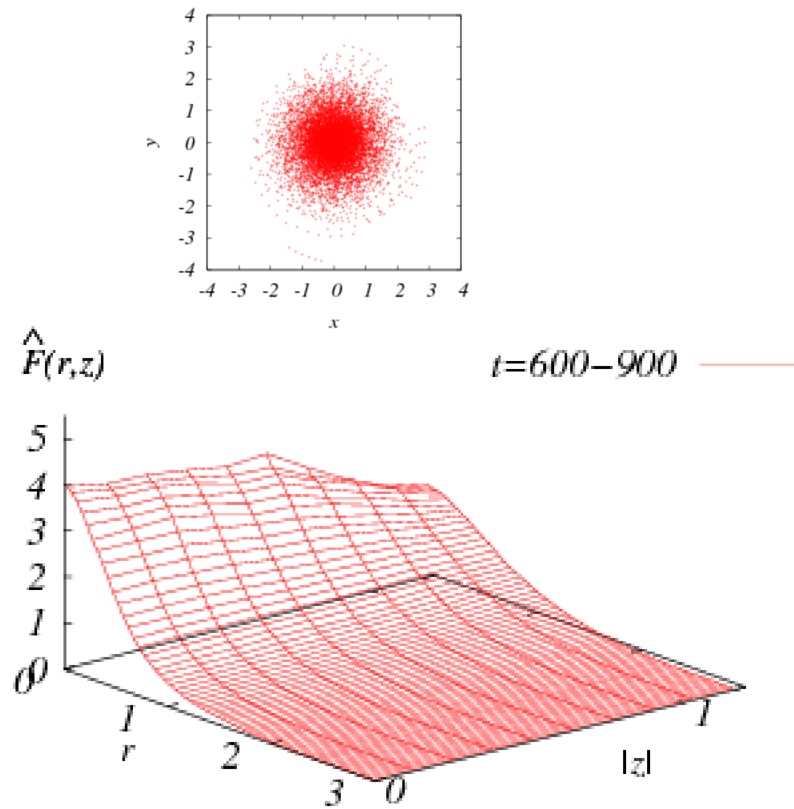

Vertical Shear: Positive Temperature

Bird View: τ=0. 20

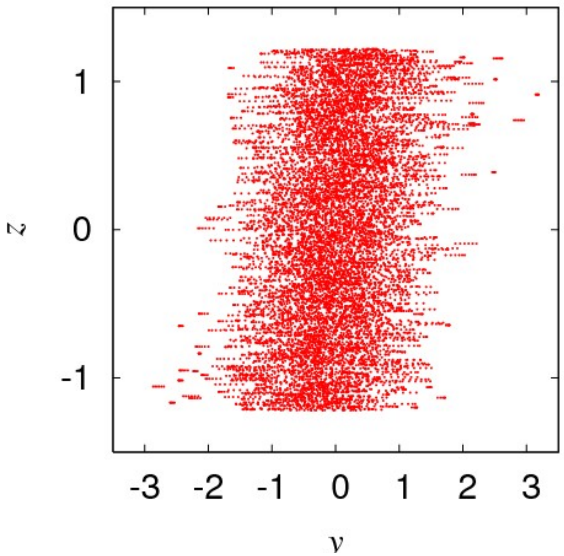

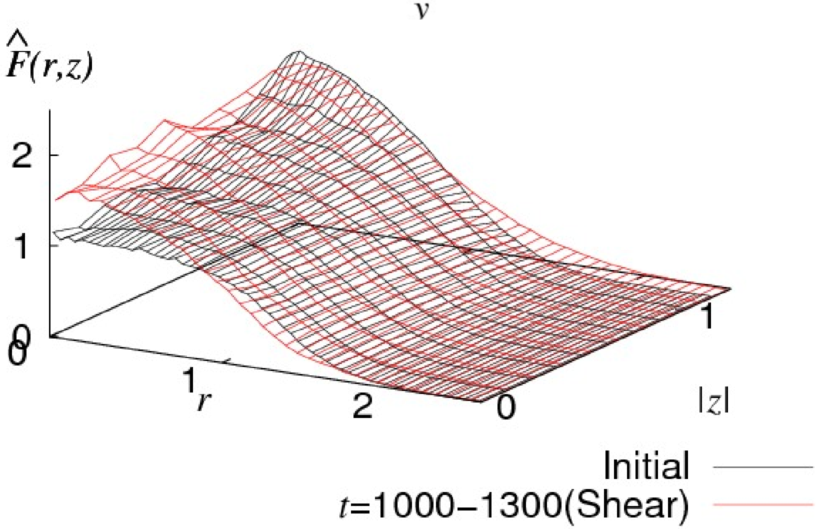

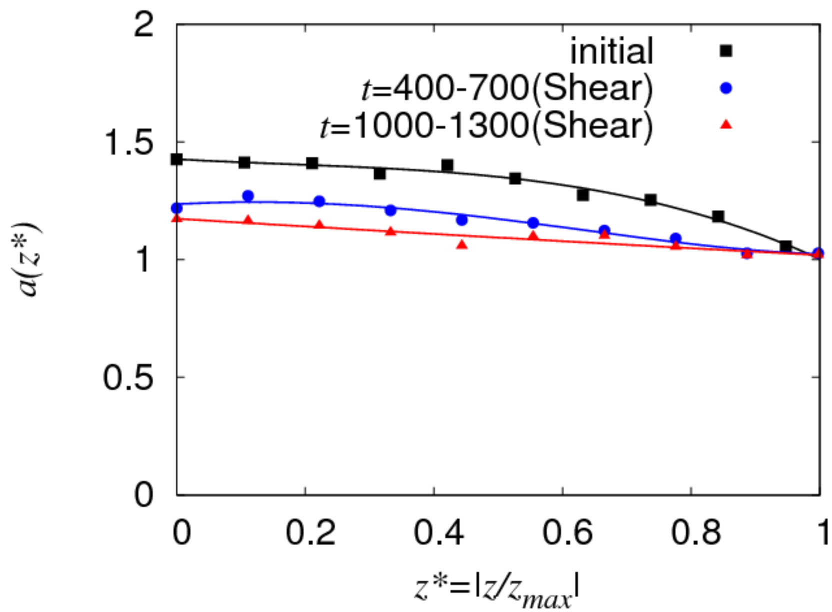

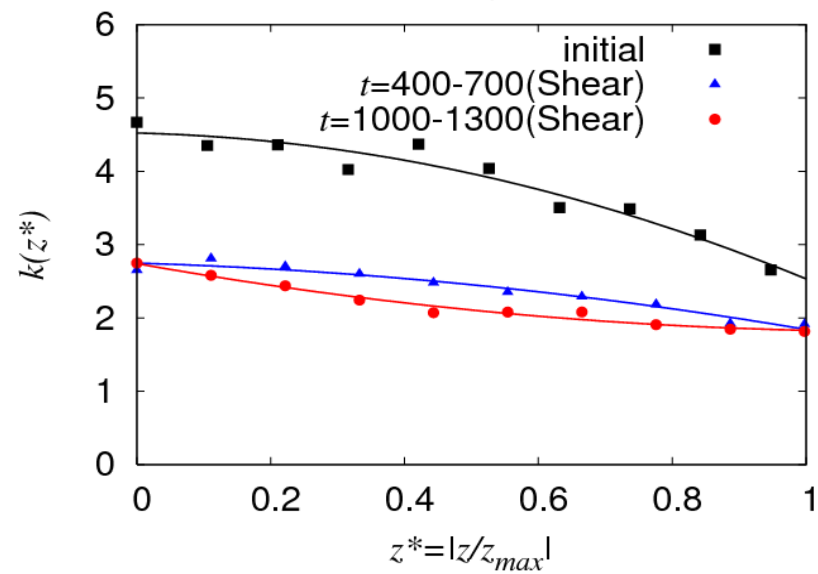

Vertical Shear: ’0’-inverse Temperature

Initial distribution :’0’-inverse temperature

Shear : *τ = 0.20*

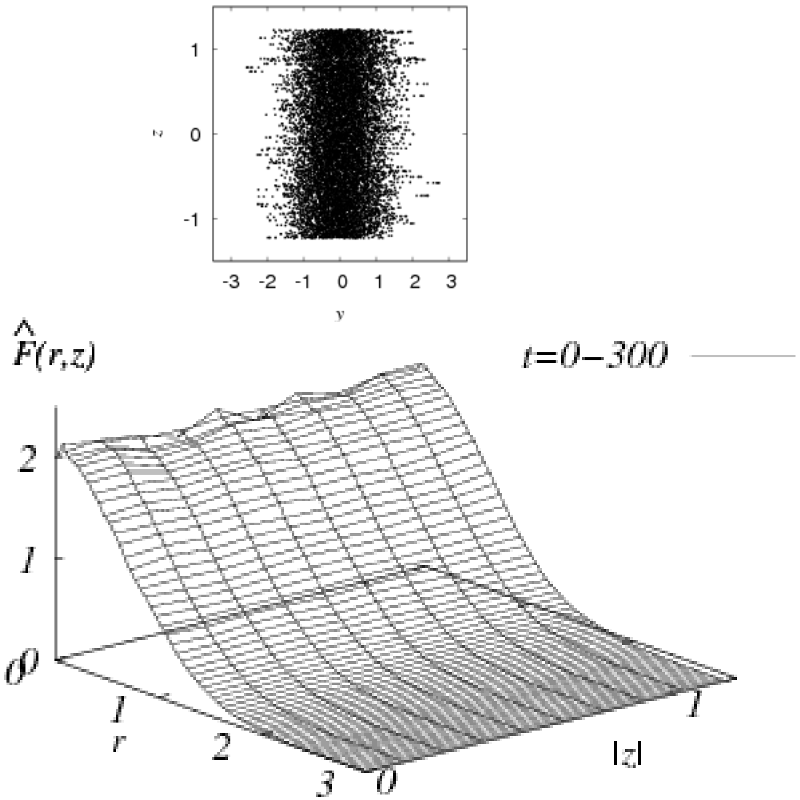

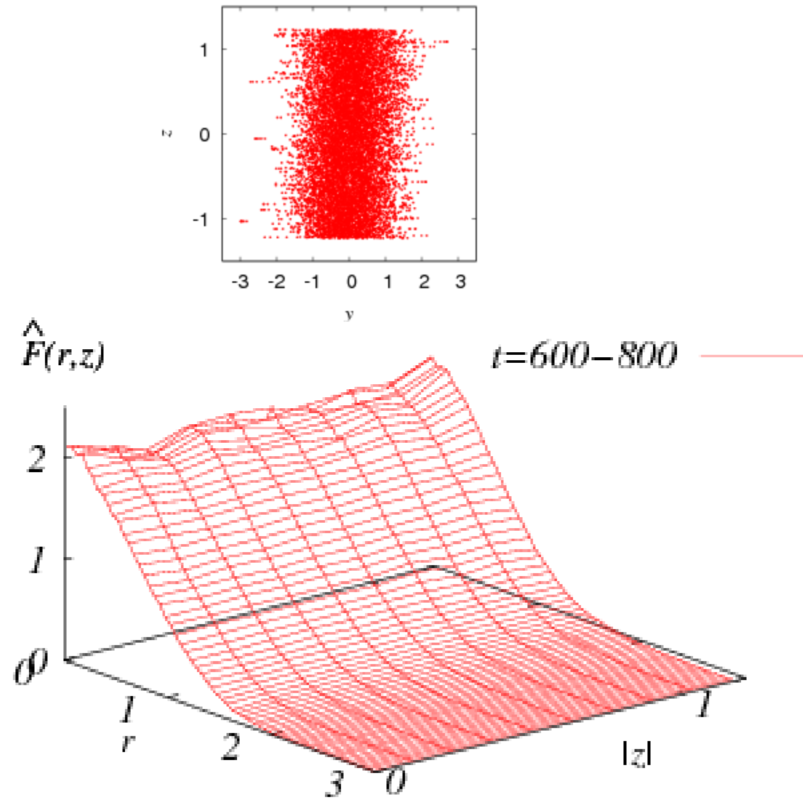

Physical Interpretation: Horizontal Strain

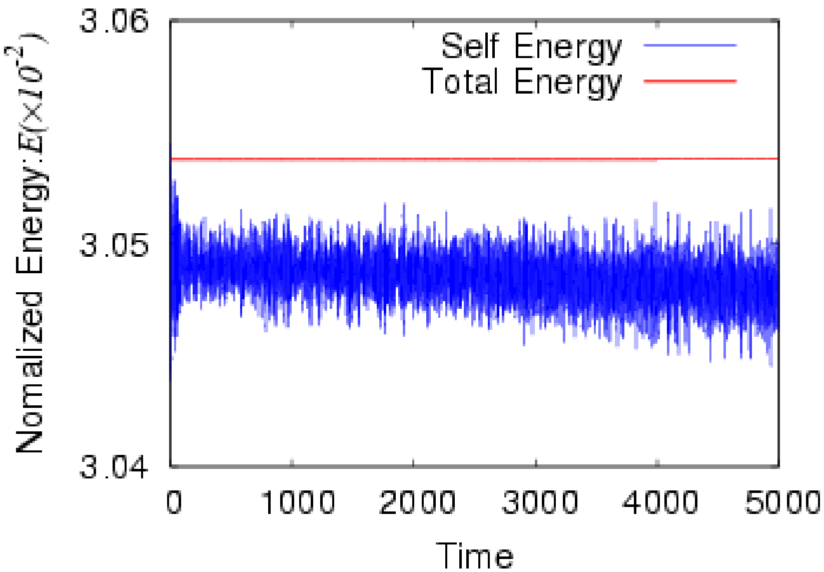

"Virtual stretching" with no change in the internal vorticity distribution will reduce the interaction energy.

VS

Little energy decrease in the actual numerical results is observed.

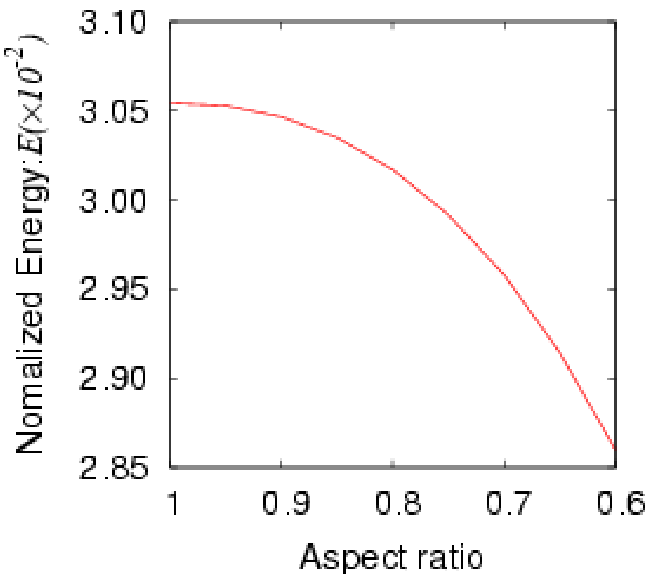

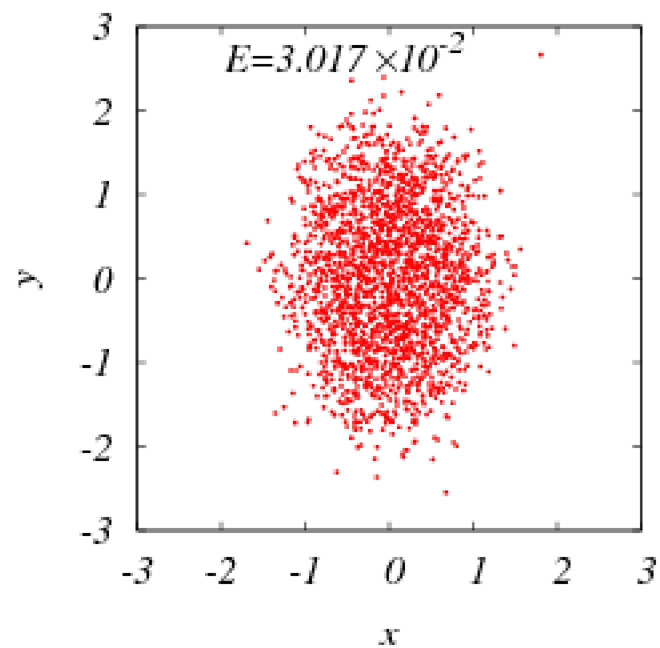

Physical Interpretation: Vertical Shear

"Virtual tilting" with no change in the internal vorticity distribution will reduce the interaction energy.

VS

Little energy decrease in the actual numerical results is observed.

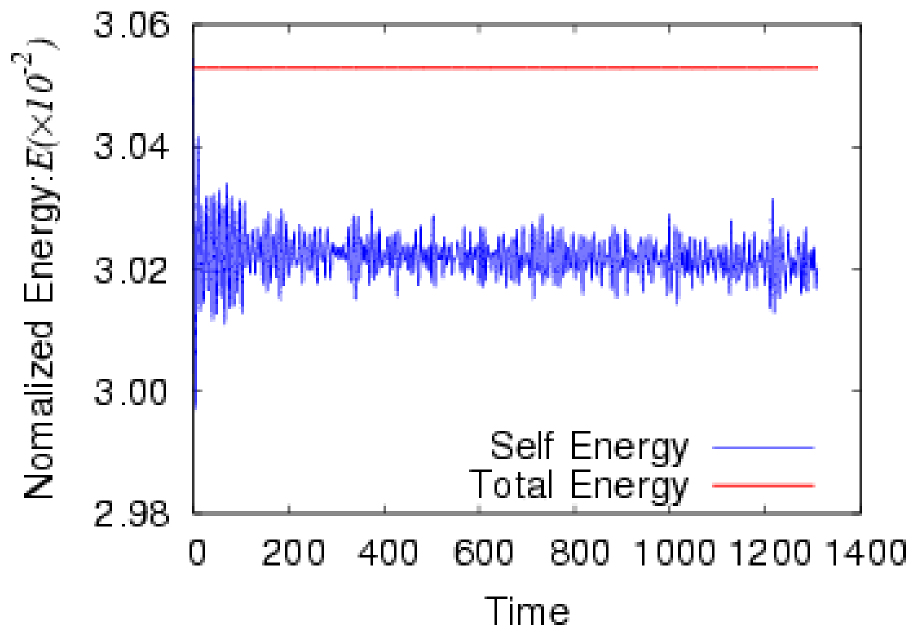

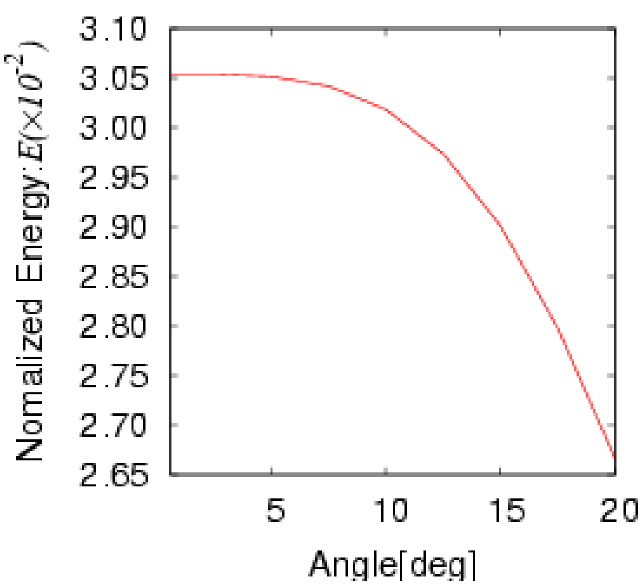

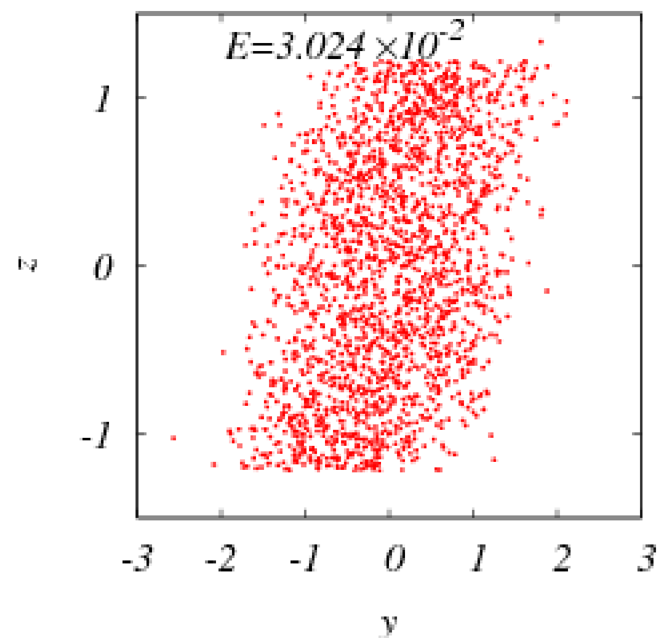

Summary

- Numerical simulations of QG point vortices and the maximum entropy theory give a consistent picture.
- Positive, 0-inverse and negative temperature states.
- “2-parameter model” is useful for parameter scanning.
- Strong interaction between vortex clouds redistributes the vorticity profile inside the clouds .
- The influence of external flow field (horizontal strain and vertical shear) on a vortex cloud is investigated. Interaction energy between vortices increases and the vorticity distribution shifts to a state of smaller inverse temperature.
- States of smaller inverse temperature are robust against external flow.

Thank you for your attention.

Acknowledgements

Dr. Hiroki Matsubara (RIKEN, Japan)
We thank for computational resources of the RIKEN Super Combined Cluster (RSCC).